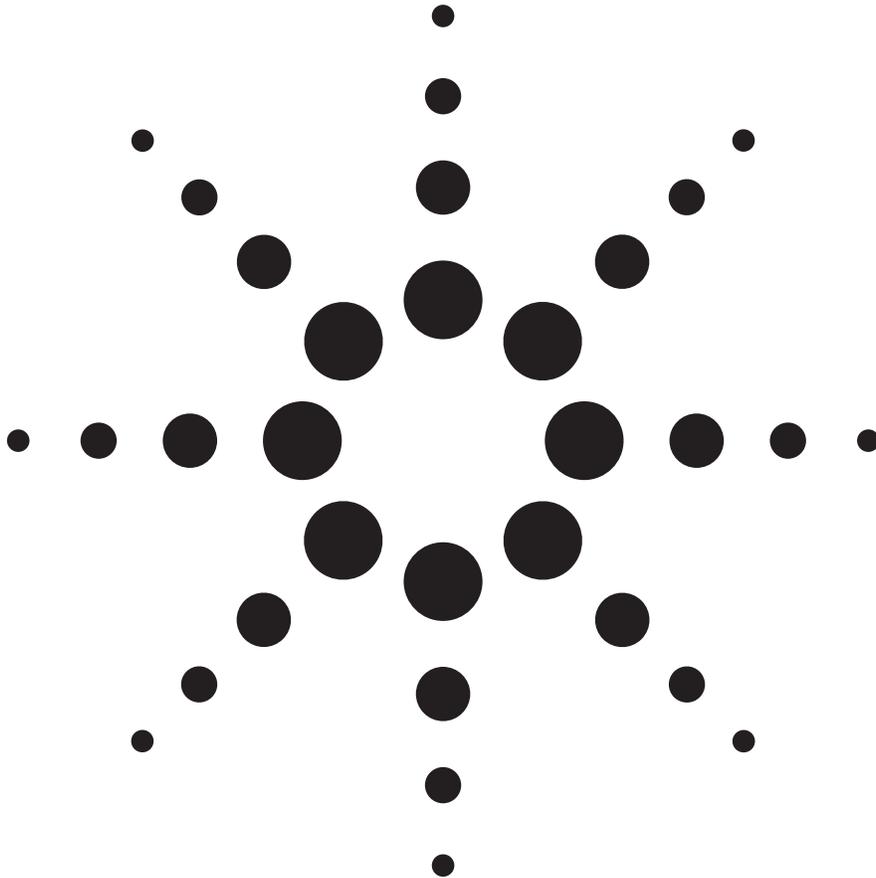# Precision Jitter Transmitter

White Paper

Agilent Technologies

Abstract

Jitter is increasingly analyzed by separating a signal's timing noise into its random and deterministic components, yet there is no reference standard for measurement verification. We introduce a precisely calibrated jitter source capable of applying a wide variety of jitter signals - Gaussian random jitter, periodic jitter (including, but not limited to, sinusoidal jitter), inter-symbol interference, and duty cycle distortion – in different combinations at adjustable amplitudes. In most cases the calibration of the jitter sources is traceable to accepted standards with uncertainties close to 1%. We describe the system, the calibration techniques, and give examples of its utility.

Introduction

The biggest problem in the analysis of jitter by separating a signal's timing noise into its sub-components is the variation of measurements performed by different jitter test-sets on a given signal. Since the variation can span several hundred percent, it is important to understand which measurement is correct and why some measurements fail. To understand the strengths of different test techniques, learn how to compare very different techniques, and to learn how to specify a jitter analyzer's accuracy and sensitivity, we built a transmitter capable of injecting arbitrary combinations of accurately calibrated levels of different types of jitter. We required that the applied jitter signals be consistent with the standard industry-wide conventions that all jitter analysis test equipment assume; for example, the random jitter signal was required to faithfully follow a Gaussian distribution over at least fourteen standard deviations.

A precision jitter transmitter is also useful for identifying problems in passive elements – backplanes, cables, connectors, applications, etc – and receivers by observing their response to known levels of different types of jitter.

The standard SONET/SDH techniques provide applied sinusoidal jitter at precisely defined levels but we are aware of no transmitter capable of transmitting precise levels of Gaussian random jitter (RJ), inter-symbol interference (ISI), and duty-cycle distortion (DCD), as well as periodic jitter (PJ). The design of a precision jitter transmitter is nontrivial: first, it is difficult to apply RJ that faithfully follows a Gaussian distribution over the range necessary to prove total jitter (TJ) at bit error ratios (BERs) of 10^{-12} or lower; and second, the calibration effort increases exponentially with the desired number of data patterns, data rates, DCD, and ISI levels.

Design Requirements

The primary design requirement was that the transmitter be calibrated, to the extent possible, with techniques that are traceable to reference standards.

The fundamental design philosophy was to provide a transmitter whose applied jitter signals were true to standard industry-wide assumptions: that RJ follows a Gaussian distribution, sources of deterministic jitter (DJ) result in bounded distributions, and that jitter is a stationary phenomenon.

We designed the transmitter to apply a wide range of different levels and combinations of RJ, PJ, ISI, and DCD that result in a large set of TJ values. The applied jitter levels are referred to in different ways depending on whether or not they result in bounded or unbounded distributions. Gaussian RJ is determined by its rms width, σ; and the sources of deterministic jitter (DJ), PJ, ISI, and DCD, are determined by the peak-to-peak spread of their distributions, indicated by DJ(p-p), PJ(p-p), ISI(p-p), and DCD(p-p). To provide a useful sub-space in a reasonable calibration effort, the precision jitter

transmitter can apply user settable levels of RJ and both sinusoidal and triangular PJ. The calibration effort intensifies as more levels of ISI and DCD are introduced because each combination must be calibrated separately.

While the calibration techniques described here can be applied at any data rate and for any repeating data pattern, we limited our efforts – again, to keep the calibration effort tenable – to a single data rate, 2.5 Gb/s, a single data pattern, a standard pseudo-random binary sequence of length 2^7-1 (PRBS7), a single pair of NRZ logic levels, and a single ended transmission line.

The precision of the applied jitter levels is limited by the intrinsic baseline jitter of the pattern generator; that is, the jitter of the transmitter in the absence of an applied jitter.

Total jitter is defined with respect to a given BER that is usually quite small, BER, We refer to it as TJ(BER) and chose to calibrate the transmitter at TJ(10^{-12}). Since the industry defines RJ to follow a Gaussian distribution, we required that the cumulative distribution function resulting from applied RJ faithfully reproduce a complementary error function to BER $\leq 10^{-12}$.

We chose levels of jitter that reflect what is common in the field. Low levels correspond to levels a network element would generate and still easily pass most standards' compliance test and high levels correspond to either barely passing or not quite passing. In most applications the dominant contributors to TJ(BER) are RJ and ISI. RJ is typically in the range $\sigma \sim 2$ to 5 ps, corresponding to TJ(10^{-12}) ~ 28 to 70 ps. ISI can vary widely; a typical 30 to 45 inch backplane trace at 2.5 Gb/s results in ISI(p-p) ~ 70 to 140 ps. For PJ it is more difficult to offer a typical value because of its source dependence. If the oscillators on a board are well shielded, then the PJ level is zero, otherwise the PJ level can be substantial. We chose PJ(p-p) levels in the range 7 to 28 ps for both sinusoidal and triangle-wave jitter.

Precision Jitter Transmitter Design

The transmitter is based on a phase modulated precision clock source driving a high bandwidth pattern generator. Random and periodic jitter are applied to the clock signal, DCD is applied by adjusting the crossing point level, and ISI is applied by transmitting the signal from the pattern generator through different lengths of printed circuit board. A few other components are included in the transmission path for impedance matching and to modify the rise/fall time of the signal. A schematic of the transmitter is given in Figure 1 and its components are described in the following sub-sections.

The vector signal generators and RJ/PJ sources

Two VSGs, Agilent E8267Cs, are combined to provide a clock signal that drives the pattern generator. Each VSG has a pair of programmable Arbitrary Waveform Generators (AWGs) that independently drive I and Q to phase modulate the clock signal. The I/Q modulation bandwidths are 160 MHz, but the programmed waveforms are sampled at 100 MS/s giving a Nyquist limit of 50 MHz. An anti-aliasing filter limits the programmable I/Q bandwidth to 40 MHz. Two VSGs are required to provide enough memory to generate an RJ signal that faithfully reproduces a Gaussian BER profile down to BER $< 10^{-12}$.

Random and Periodic Jitter (RJ and PJ) are generated using Agilent's Signal Studio Jitter Injection software [1]. The phase modulation terms are defined mathematically and used to drive internal arbitrary waveform generators (AWG) in the VSGs. The PJ waveforms must be generated so that their length is an integer multiple of complete cycles of the repeating waveform. For RJ, long random sequences are generated by a MatLab [2] Gaussian random number generator. Separate sequences are applied to each of the two VSGs. The sequences consist of approximately one million points each but with slightly different lengths. To assure that there is no correlation between the waveforms, different initial seeds are used for each random sequence. The I/Q modulation of one VSG drives that of the other to mix the complete RJ signal. The modulation is filtered with a raised cosine filter at 40 MHz to prevent incidental amplitude noise. The filtered Gaussian width, σ, is calculated from the filtered waveform and the numbers are scaled to restore the desired signal level. It is the limited AWG memory that necessitates the combination of two VSGs to provide a faithful RJ signal. Both VSGs generate RJ signals, but only one is needed for the PJ signal.

The modulated clock signal drives the pattern generator so that the data generated includes RJ and PJ. The unmodulated clock output can be used to trigger a BERT error detector or a sampling oscilloscope for analyzing the modulated signal.

The pattern generator, DCD source, and transmission path

The Agilent N4901B 500 Mb/s to 13.5 Gb/s SerialBERT is used for pattern generation. The signal output has a transition time less than 25 ps and an adjustable crossing point. DCD was applied by adjusting the crossing point level.
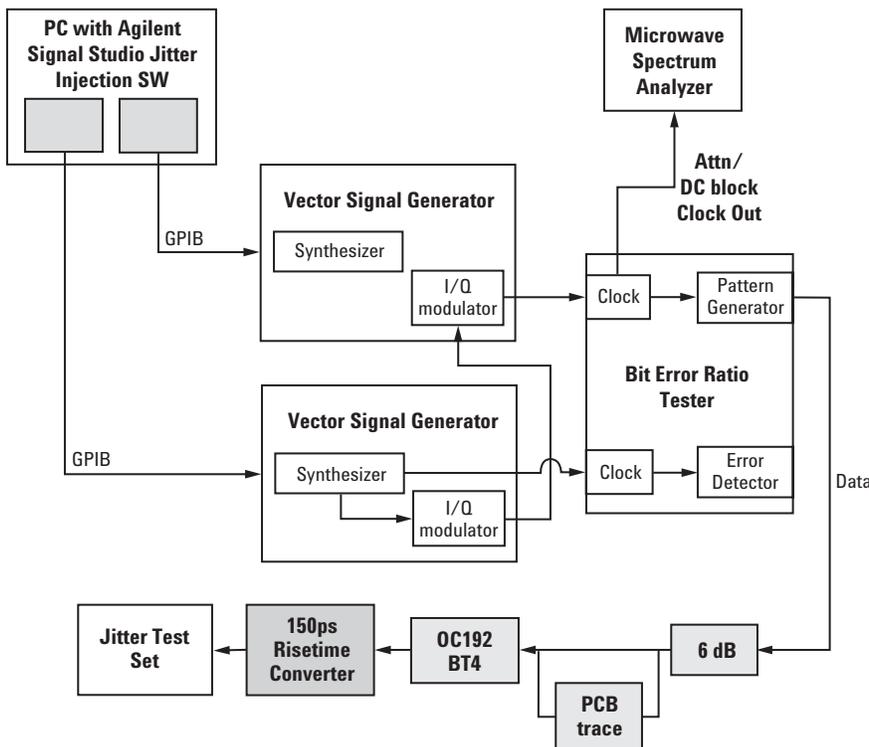

Figure 1: Schematic of the transmitter.

The data signal transmission path, those elements (independent of the PCB trace, ISI source) between the pattern generator and the jitter test-set or component being stressed, consist of a 6 dB attenuator, a 150 ps rise-time converter and a 7.5 GHz, four-pole, low-pass Bessel filter. The 6 dB attenuator was included to reduce signal reflections back to the pattern generator and the combination of the 150 ps rise-time converter and low pass filter were included to slow down the abrupt 25 ps rise/fall time of the pattern generator output and better represent a typical 2.5 Gb/s signal.

The logic voltage levels were set at the pattern generator so that the desired levels are achieved at the output of the transmission path; the '1' level was set to 600 mV and '0' level to –620 mV giving +280 mV and –280 mV respectively at the end of the transmission path. Similarly, the crossing point was adjusted to 45% to insure that the baseline signal had zero DCD.

Calibration of Applied Jitter Signals

The independent jitter signals are calibrated separately and combined into the desired combinations. The key to calibration is distinguishing those jitter signals that are independent from those that interfere with each other. RJ is independent of all sources of DJ; PJ is independent of the other sources; and DCD and ISI are independent of the other sources, but not independent of each other. Thus the independent sources that must be calibrated are RJ, PJ, and all combinations of DCD*ISI. Additionally, the baseline of the transmitter itself – that is, the transmitted signal in the absence of any applied jitter signal – must also be calibrated.

Given the calibration constants for each jitter source, the level of jitter for any configuration of RJ, PJ, ISI, and DCD, as well as their uncertainties, can be calculated. Since the RJ levels from each source and their uncertainties are independent, the total RJ of a given signal is the root-square-sum (rss) of the components,

$$\sigma_{Total} = \sqrt{\sigma_1^2 + \sigma_2^2 + \ldots + \sigma_n^2}. \qquad (1)$$

Since the peak-to-peak value of the convolution of two independent bounded distributions is given by the sum of the individual peak-to-peak values, the peak-to-peak value of a combination of independent DJ sources is simply the sum of the bounded peak-to-peak values,

$$DJ_{Total}(p\text{-}p) = DJ_1(p\text{-}p) + DJ_2(p\text{-}p) + \ldots + DJ_N(p\text{-}p). \qquad (2)$$

The uncertainties in the calibrated values must also be combined to give the net uncertainty of the applied signal. If it is not known whether a given uncertainty is independent of another, then they must be combined with the worst-case assumption that they are 100% correlated; in which case they are added together. While the DJ signals are independent, their uncertainties may not be. The DJ uncertainties tell us not just, for example, how far off the calibrated baseline signal might be, but how much of the baseline signal might be manifest as ISI or DCD.

For each independent jitter source, RJ, PJ, ISI, DCD, and the combinations of ISI_DCD, there are, in principle four calibration constants: RJ (σ), the uncertainty in RJ ($\delta\sigma$), DJ(p-p) and the uncertainty δDJ(p-p). The calibrations are summarized in Table 1.

Table 1: Calibration summary. *The meaning of "low" and "high" levels of DCD are given in the text.

Baseline	σ_{base} = 0.685 ps, $\delta\sigma_{base}$ = 0.270 ps, $DJ_{base}(p\text{-}p)$ = 3.7 ps, $\delta DJ_{base}(p\text{-}p)$ = 1.0 ps
RJ	$\sigma = \sqrt{(\sigma_{applied}^2 + 0.270^2)}$, $\delta\sigma$ = 0.270 ps + 1.5%x$\sigma_{applied}$
PJ	$\delta PJ(p\text{-}p)$ = 1%xPJ(p-p)
DCD	$\delta DCD(p\text{-}p)$ = 0.8 ps + 0.5%xDCD(p-p) for "low"* levels of DCD
	$\delta DCD(p\text{-}p)$ = 0.2 ps + 0.5%xDCD(p-p) for "high"* levels of DCD
ISI	$ISI(p\text{-}p) = ISI_{applied}(p\text{-}p)$ + 3.7, $\delta ISI(p\text{-}p)$ = 1.0 ps + 2%xISI(p-p)
ISI*DCD	$\delta(ISI*DCD)$ = 0.8 ps + 2 %x(ISI*DCD)

Calibration of the transmitter baseline random jitter

The transmitter baseline jitter is the jitter of the precision transmitter in the absence of an applied jitter signal. The baseline configuration is given, in Figure 1, by the case where no phase modulation is applied to the VSG clock signal driving the pattern generator, the DCD level is tuned to zero, and the transmission path includes the filters and transition time converter but no backplane. Extensive use of an equivalent time sampling oscilloscope, the Agilent 86100 Digital Communications Analyzer (DCA) with a wide-bandwidth electrical receiver (e.g., 86117A) and precision time-base (Agilent 86107A) is necessary for baseline calibration – since the advanced jitter analysis capabilities of the DCA-J are one of the subjects to study with the precision jitter transmitter, absolutely no use of its jitter analysis ability were used in calibration; the entire calibration process was performed prior to making any observations with jitter test-sets.

Data is accumulated on the DCA with the time and voltage scales tuned for maximum resolution of the crossing point under three different configurations: the unmodulated clock signal is split so that identical full data-rate clock signals serve as both the trigger signal and the data signal. Since the jitter distribution recorded by the DCA is the relative jitter between the trigger signal and the data signal, the split-clock configuration has zero signal jitter. Thus the jitter observed on the DCA must be the intrinsic jitter, or noise floor, of the DCA and precision time-base. We measured a noise floor of 0.270 ps.

In Figure 2a the unmodulated clock signal is used to trigger the DCA on an alternating (e.g., 101010) pattern including the transmission path. A Gaussian distribution was fit to the alternating pattern crossing-point histogram, yielding a width of $\sigma = 0.736$ ps. Since the distribution is consistent with a Gaussian, we conclude that the jitter on the alternating pattern has negligible DJ. Since the DCA intrinsic jitter is independent of the jitter on the alternating pattern, it can be subtracted from the RJ baseline in the usual way [3], $\sigma_T^2 = \sigma_{split-clock}^2 + \sigma_{PG}^2$. The precision jitter transmitter baseline RJ, independent of the DCA intrinsic RJ, is $\sigma = 0.685$ ps. The intrinsic noise also indicates the fluctuations that would be experienced if we could repeat the measurement on many different systems; that is, the intrinsic noise indicates the systematic uncertainty of our technique. Since Gaussian RJ is fundamentally a thermal phenomenon, we assume that the generation of a pattern with more structure than the alternating pattern does not introduce any additional RJ, therefore,
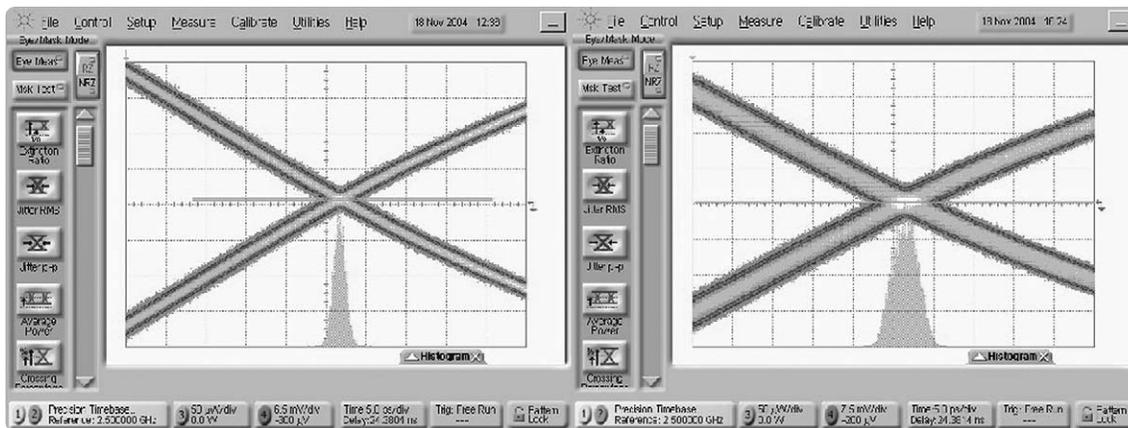
$$\sigma_{base} = 0.685 \pm 0.270 \ ps. \qquad (3)$$

Figure 2: Examples of data accumulated for analyzing the baseline jitter, (a) an alternating, 101010, pattern; and (b) the baseline PRBS7 pattern.

Calibration of the transmitter baseline deterministic jitter

The baseline DJ of the pattern generator is composed of the convolution of the ISI contributed by the transmission path and the ISI of the pattern generator. The baseline ISI can be calculated from the combination of its frequency response – which is obtained by measuring its S-parameters – and the averaged waveform of the PRBS7 pattern. First the S-parameters of the transmission path (cables connectors, filters, pad) are measured on a 20 GHz vector network analyzer; then a PRBS7 pattern waveform is captured on a DCA. The impulse response of the pattern generator, which can differ in generating a pattern as opposed to a single step, is calculated by taking the Fourier transform of the pattern waveform and dividing it by the Fourier transform of an ideal PRBS7 pattern. The product of the spectral behavior of the transmission path and pattern generator impulse response is transformed to the time domain with an inverse Fourier transform to obtain the system impulse response which is convolved with an ideal PRBS7 pattern to get the ISI distribution. Calculating ISI(p-p) from the ISI distribution is straightforward and yields a baseline ISI(p-p) = 4.7 ps. The uncertainty of the calculation is less than 2% and as we'll see, is negligible for the baseline DJ(p-p) calibration.

The baseline RJ was convolved with the calculated ISI to give a prediction for the baseline jitter distribution on a PRBS7 signal, Figure 2b. The calculated and measured baseline eye-diagrams are presented in Figure 3 and show remarkable consistency. The crossing point histograms, or jitter distributions, are shown in Figure 4; while qualitatively similar, they are not quite statistically consistent. To compare the calculated baseline ISI(p-p) with the DJ observed in the baseline data we used a method that builds on the dual-Dirac model [4]. First, the dual-Dirac technique is applied to the baseline jitter distribution shown in Figure 2b and Figure 4. To properly implement the dual-Dirac model, the jitter distribution is integrated to yield the Cumulative Distribution Function (CDF) and the complementary error function is fit to the tails below a BER threshold, in this case 10^{-3} – since the DJ is very low on the baseline, 10^{-3} is an adequate threshold, but all that matters here is that the complimentary error function give a good fit. Second, the dual-Dirac model is applied – in precisely the same way – to a set of distributions calculated by convolving the ISI of the transmission path with Gaussian distributions having different values of σ. Third, the ratio $DJ(\delta\delta)/\sigma_{fit}$, derived from the dual-Dirac model applied to the calculated distributions is plotted against the ratio of the transmission path ISI and convolved RJ widths, $DJ(ISI)/\sigma$. The $DJ(\delta\delta)/\sigma_{fit}$ ratio from the baseline data is then translated from the dual-Dirac assumption to the transmission path ISI assumption to yield $DJ(ISI)/\sigma$ which is then multiplied by the measured RJ of Eq. (3) to get our best estimate for the baseline DJ(p-p), 3.7 ps.

Since the ISI of the transmission path can interfere with the ISI of the pattern generator, the transmission path ISI is not necessarily a lower limit for the baseline ISI.

But it does give an independent estimate of DJ(p-p). Thus, the systematic uncertainty in DJ(p-p) is given by the difference of the calculated transmission path ISI and the best estimate for DJ(p-p), thus

$$DJ_{base}(\text{p-p}) = 3.7 \pm 1.0 \text{ ps.} \qquad (4)$$

Calibration of periodic jitter

Periodic jitter is any type of regularly repeating jitter signal. It is not generally correlated to the repetition rate of the data pattern and so falls in the category of uncorrelated jitter. We calibrated two types of PJ. Sinusoidal jitter introduces a phase term,

$$\phi(t) = A_{PJ} \sin(2\pi f_{PJ} t)$$

where A_{PJ} is the amplitude of the jitter signal in UI, or seconds, and f_{PJ} is the frequency of the applied jitter. Applying PJ through I/Q modulation of the VSG clock signal is trivial for sinusoidal jitter, a fixed amplitude and frequency. For triangular jitter it is slightly more challenging, the Fourier series representation of the triangle wave provides the amplitudes, frequencies and phase offsets up to the bandwidth of the modulator – here about 40 MHz.
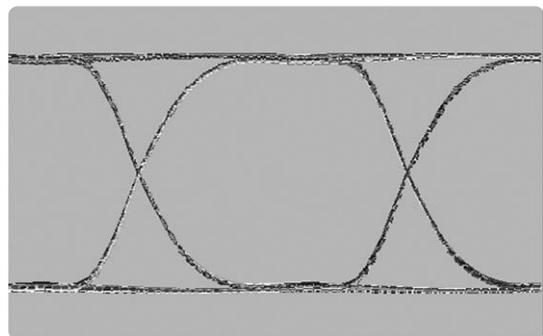
(a)
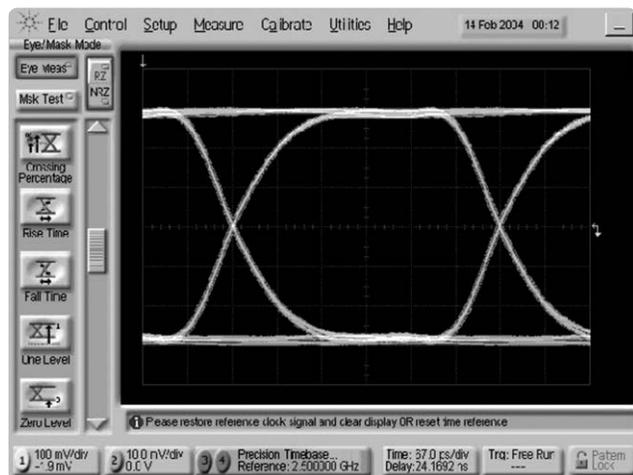
(b)

Figure 3: Comparison of the measured baseline eye diagram, (a), with the eye diagram calculated from the frequency response of the transmission path, time-averaged impulse response of the pattern generator on a PRBS7 and the observed baseline RJ.
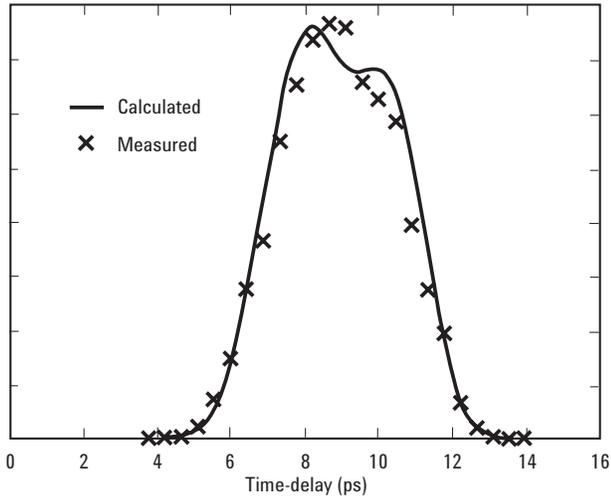
Figure 4: The calculated (solid) and measured (crosses) jitter distributions of the baseline transmitter.

Our sinusoidal periodic jitter signal was set at 15 MHz and its amplitude was calibrated with a slight variation of the standard Bessel null technique used in SONET/SDH applications [5]. First, an alternating pattern was transmitted from the pattern generator at 2.5 Gb/s (i.e., a 1.25 GHz square wave) and the output was observed on a spectrum analyzer. Phase modulation theory predicts a null at the carrier frequency for a modulation amplitude of 0.765488 UIp-p. Since the serial data specifications' jitter budgets are much smaller than this, we checked the calibration at an amplitude of 0.765488/7.5 = 0.102065 UI. At this amplitude, the theory predicts a null at the 15th harmonic, 18.75 GHz. The programmed modulation level required to obtain $20*\log(J_1/J_0) > 33$ dB was recorded for the 15 MHz modulation frequency, as shown in Figure 5, and included in the calibration table. The > 33 dB limit corresponds to less than ±1% deviation error.

Our triangular PJ signal was set to 2 MHz. Calibration of the triangular PJ relies on the same I/Q modulation accuracy as the sinusoidal PJ signal. The difference is that the signal has up to twenty harmonic frequencies but the fundamental linearity of the amplitude and frequency applied to the I/Q modulators is the same as that confirmed at a single frequency for the sinusoidal PJ. The Bessel Null technique was applied to sinusoidal signals at seven different frequencies (1, 5, 10, 15, 20, 25, and 30 MHz) to confirm I/Q consistency across the modulation bandwidth. The calibration of the resulting triangular PJ amplitude was confirmed by applying the modulated clock to a phase detector and observing the output on an Infinium real-time oscilloscope. The peak-to-peak value of the 2 MHz triangle wave was compared to that of a 2 MHz sinusoid of the same programmed value. A variation of no more than 0.5% beyond the % deviation error of the sinusoidal jitter calibration was observed.

Since the baseline RJ includes the clock RJ, there is no RJ component included in the PJ signal. Further, the calibration of the transmitter baseline indicates that the baseline DJ is dominated by DDJ, so there is no additive PJ uncertainty. Thus for sinusoidal PJ, $\delta PJ(p\text{-}p) = 1\% x PJ(p\text{-}p)$ and for triangular PJ, $\delta PJ(p\text{-}p) = 1.5\% x PJ(p\text{-}p)$.
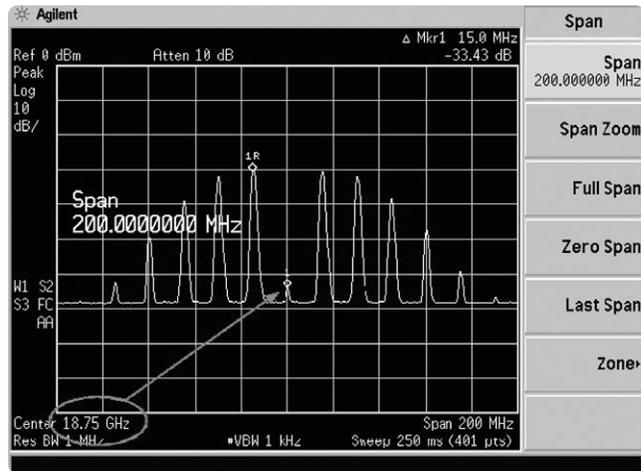

Figure 5: The Bessel null of the 15th harmonic.

Calibration of Random Jitter

We required that the RJ source have an incoherent phase modulation spectrum and faithfully follow a Gaussian distribution with tails extending over fourteen standard deviations so that it would conform to the industry convention down to TJ(BER = 10^{-12}). Strictly maintaining an RJ signal that follows a Gaussian distribution is also important for comparing jitter test-sets because different techniques make the Gaussian assumption in different ways.

RJ was introduced to the clock signal the same way as the PJ signal, by programming set phase modulation terms. In the RJ case the terms are a set of random numbers that follow a Gaussian distribution. These values are then filtered with a 40 MHz raised cosine filter and renormalized to the desired standard deviation. The uncertainty in this technique is dominated by the same uncertainties as the applied PJ signals. The differences in calibrating RJ compared to PJ is that the Bessel null technique has to be repeated across the full RJ bandwidth to account for the accuracy of each frequency component of the RJ signal thrown to the I/Q modulators. The Bessel null technique was applied to seven different sinusoidal jitter frequencies (1, 5, 10, 15, 20, 25, and 30 MHz) and the variation of the set amplitudes with the Bessel Null calibrations provides the uncertainty in the variation of the I/Q modulator's frequency response. That RJ faithfully follows a Gaussian down to BER of 10^{-12} is demonstrated in Figure 6.

The RJ applied to the clock signal convolves with the intrinsic RJ of the pattern generator, 0.685 ps. The uncertainty of the baseline, 0.270 ps, provides an additive constant to the total RJ uncertainty. The applied RJ uncertainty is $\delta\sigma$ = 0.270 ps + 1.5%x$\sigma_{applied}$.

Analysis of the RJ signal similar to that performed in the transmitter baseline calibration indicates that there is no DJ applied by the RJ source beyond that of the baseline transmitter.

Calibration of duty-cycle distortion

Duty Cycle Distortion (DCD) is defined as the average difference of the crossing time of rising and falling edges – it is therefore a signed quantity

$$DCD(\text{p-p}) \equiv \overline{x}_{rise} - \overline{x}_{fall}.$$

DCD is calibrated by acquiring a histogram of the crossing point on a DCA. With only DCD applied, the jitter distribution is bimodal. The difference in the means of the lobes yields the DCD level. In the "low" DCD cases where the two lobes overlap, the averages are calculated by fitting Gaussian distributions separately to each peak. For the "high" DCD cases where the distributions are separate, the averages can be calculated directly from the two separate distributions. The uncertainty of the "low" DCD conditions where fits are required is about 0.8 ps – based on the fitting uncertainty. The uncertainty in the "high" DCD cases is the standard deviation of the mean, about 0.2 ps. The total uncertainty must also include the DCA timebase uncertainty of about 0.5% giving, for the "low" cases, δDCD(p-p) = 0.8 ps + 0.5%xDCD(p-p) and for the "high" cases δDCD(p-p) = 0.2 ps + 0.5%xDCD(p-p).
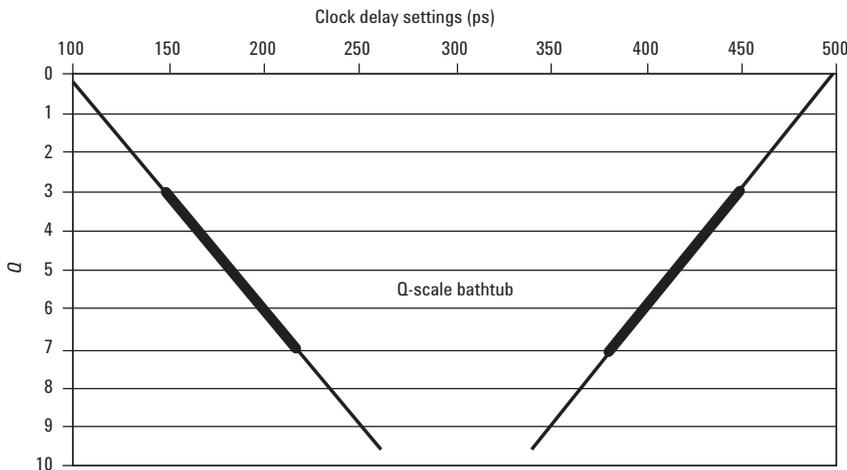

Figure 6: Graph of an applied RJ signal on a Q-scale. That the data is a straight line down to a value of Q less than 7 indicates Gaussian behavior down to BER less than 10^{-12}.

Calibration of inter-symbol interference

ISI is introduced by inserting different lengths of traces on Printed Circuit Board (PCB) into the transmission path. The effect of temperature and humidity on the PCB and transmission path is believed to be negligible because it is built from standard FR4 multilayer processing, has been kept in a controlled low humidity environment and there is no evidence for a hydroxyl absorption peak in its frequency response spectrum.

The applied ISI is calculated by including the frequency response of the different lengths of backplane in the calculation described above in the discussion of the baseline DJ(p-p) calibration. The uncertainty of the S-parameters, as measured on a PNA, are given by the worst-case tilt numbers of (0.2 dB)/(20 GHz) which changes the ISI by no more than 0.5%. We checked the accuracy of using a 20 GHz analyzer by calculating the ISI on successively smaller bandwidths. No appreciable difference was observed until the bandwidth approached twice the data rate. The uncertainty from the pattern waveform contributes another 0.5% due to the time-base accuracy of the DCA. The baseline DJ is dominantly ISI, and so the uncertainty in the baseline belongs here, resulting in a total systematic uncertainty in ISI of δISI(p-p) = 1 ps + 1%xISI(p-p).

Calibration of ISI*DCD combinations

Introduction of DCD changes a signal's frequency content. Since ISI is caused by the non-uniform frequency response of the channel, introduction of DCD changes the ISI level. In other words, ISI and DCD are correlated and every combination of ISI and DCD must be separately calibrated.

Combinations of ISI_DCD are calibrated by including the frequency response of the DCD signal in the calculation of ISI described above. It's worthwhile to notice that the levels of DCD and ISI within the ISI*DCD combinations are not the same as they are when applied separately, nor do the pair sum to the net peak-to-peak jitter – which is just another way of saying that ISI and DCD are correlated.

Calibration of total jitter at BER = 10^{-12}

Total Jitter at a BER of 10^{-12} was calculated by convolving the jitter distributions of each applied condition and then integrating the resulting distributions to determine the values of the time-delay where BER = 10^{-12} [6]. The results of the calculation are compared to the TJ results from measurements with a full BERTscan in Figure 7 for a representative subset of combinations of different jitter signals. There is excellent agreement with the calculated and measured TJ values. One expects a large positive fractional error for low uncertainties due to the effects of the BERT error detector sensitivity and the small intrinsic uncertainty in the BERT time-delay. The uncertainty of TJ is calculated by propagating the uncertainties of each independent source of jitter through the TJ calculation, we typically achieve δTJ(10^{-12}) = 5 ps.
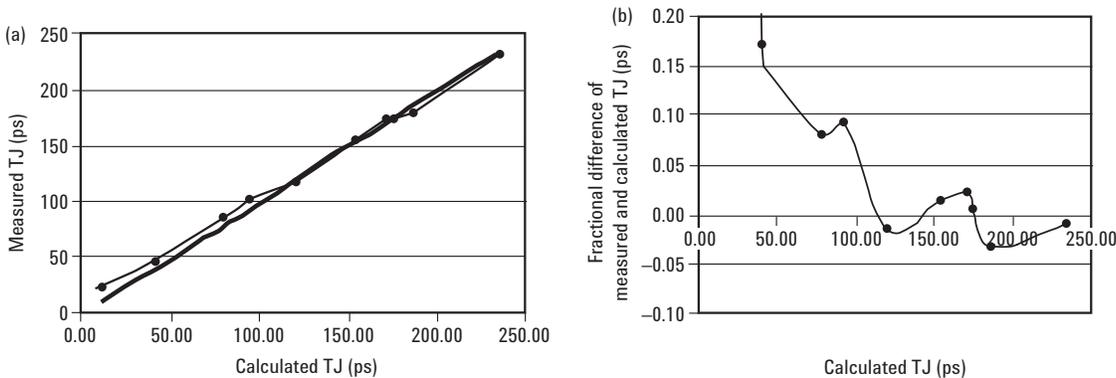

Figure 7: Comparison of TJ(10^{-12}) calculated from the various RJ/DJ calibrations with measurements performed on a BERT. In (a) the measured TJ is plotted against the calculated values, the straight line would correspond to perfect agreement; in (b) the fractional difference between the calculated and measured values of TJ show agreement of better than 10% that can be accounted for by intrinsic uncertainties in the BERTscan technique.

Transmitter Stationarity

One of the implicit industry-wide assumptions about jitter is that it is a stochastically stationary phenomenon. In other words, measurements that are performed over a time duration long enough to include both RJ and DJ phenomena are equivalent, up to random fluctuations, regardless of the time that they are performed. While there was no reason to believe that the precision jitter transmitter would experience non-stationary events, several tests were performed to assure stationarity. An example of a non-stationary event would be a rare transient phenomena such as an unaccounted for burst of jitter. The precision jitter transmitter was monitored for two hours with high levels of applied of ISI and DCD on an Agilent 54855A real-time oscilloscope using EZJIT software to acquire a jitter distribution and frequency spectrum. The process was repeated several times and no rare random processes were observed. We conclude that the precision jitter transmitter is at worst stationary over the vast majority of two hour periods – certainly sufficient for consistence with the industry assumptions.

Conclusion

The precision jitter transmitter can be assembled from readily available instruments. The application of jitter injection software using the I/Q modulation of the vector signal generators greatly simplifies the application of truly Gaussian random jitter and periodic jitter of various shapes. To maintain RJ with Gaussian tails corresponding to BER=10^{-12}, it is necessary to use two vector signal generators. In the development of the precision jitter transmitter we tried several instrument grade noise sources applied to the pattern generator time-delay, none of the noise sources produced a jitter distribution consistent with a Gaussian at the level of BER = 10^{-12}.

Calibration of RJ, PJ, ISI, DCD, and combinations of ISI and DCD are all traceable to calibration standards and were accurate to levels of a few percent.

Calibration of the baseline RJ is not traceable to a calibration standard, however its magnitude is small and, as a percentage, its systematic uncertainty is large. The uncertainty in the baseline RJ propagates through the as an additive constant in the uncertainty of applied RJ signals. The baseline RJ uncertainty also propagates into the calibration of TJ(10^{-12}) as a substantial, but unavoidable, uncertainty. Similarly, the calibration of the baseline DJ is only partially traceable and has large uncertainties. That the untraceable constituents of the jittered signal have the largest uncertainties is not a coincidence; rather, it reflects the general difficulty of separating a signal into components without some a prior knowledge of their functional form.

In jitter analysis the important observables are TJ(BER), RJ, PJ, ISI, DCD, and DDJ, not DJ(p-p). An often overlooked subtlety of the ubiquitous dual-Dirac model is the fact that the value of DJ it extracts, DJ($\delta\delta$) is not an estimator of the actual peak-to-peak DJ (4). In fact, for realistic jitter distributions, DJ($\delta\delta$) < DJ(p-p) (it should be noted that the same is not true of RJ, the width of the RJ Gaussian, σ, is an estimator for the parameter RJ in the dual-Dirac model – though the fitting techniques tend to yield $\sigma_{fit} \leq \sigma$). But, in fact, the actual peak-peak DJ has no utility; independent of the actual DJ distribution, DJ(p-p) is helpful for neither estimating TJ(BER) - where DJ($\delta\delta$) is needed – nor as a diagnostic tool – where PJ, ISI, DCD, and DDJ are helpful.

Finally, the precision jitter transmitter can be used for several sensitive applications. We developed it to study the variations of different jitter analysis techniques under a given condition, to understand what techniques are most effective, and to learn how to specify jitter accuracy and sensitivity. The results of that study are beyond the scope of this paper, but are available in reference 7.

[1] Timothy Peters, *E4438C-SP1 Signal Studio For Jitter Injection*, details available at **www.Agilent.com**.

[2] **www.mathworks.com**.

[3] For a thorough discussion of the compensation of timing errors in this type of measurement, see Paul Hale, C.M. Wang, Dylan F. Williams, Kate A. Remley, and Joshua Wepman, *"Compensation of Random and Systematic Timing Errors in Sampling Oscilloscopes,"* submitted to IEEE Trans. Instr. Meas.; another useful reference is T.M. Souders, D.R. Flach, C. Hagwood, and G.L. Yang, *"The effects of timing jitter in sampling systems,"* IEEE Trans. Instrum. Meas., vol. 39, pp. 80-85, 1990.

[4] Ransom Stephens, *"Jitter Analysis: Q-scale, the dual-Dirac model and RJ/DJ,"* Agilent Technologies Whitepaper, 2004. Available from **www.Agilent.com**.

[5] Agilent Tutorial, *"Understanding Jitter and Wander Measurements and Standards, Second Edition,"* Agilent Literature number 5988-6254EN, 2003. Available from **http://cp.literature.agilent.com/litweb/pdf/5988-6254EN.pdf.**

[6] There are many summaries of the definition of TJ(BER), see, for example, Ransom Stephens, *"Analyzing Jitter at High Data Rates,"* IEEE Optical Communications Testing, February 2004.

[7] Ransom Stephens et al., *"Comparison of different jitter analysis techniques with a precision jitter transmitter,"* Agilent Technologies Whitepaper 2005. Available from **www.Agilent.com**.

11

www.agilent.com
www.agilent.com/find/dca

Agilent Technologies' Test and Measurement Support, Services, and Assistance
Agilent Technologies aims to maximize the value you receive, while minimizing your risk and problems. We strive to ensure that you get the test and measurement capabilities you paid for and obtain the support you need. Our extensive support resources and services can help you choose the right Agilent products for your applications and apply them successfully. Every instrument and system we sell has a global warranty. Two concepts underlie Agilent's overall support policy: "Our Promise" and "Your Advantage."

Our Promise
Our Promise means your Agilent test and measurement equipment will meet its advertised performance and functionality. When you are choosing new equipment, we will help you with product information, including realistic performance specifications and practical recommendations from experienced test engineers. When you receive your new Agilent equipment, we can help verify that it works properly and help with initial product operation.

Your Advantage
Your Advantage means that Agilent offers a wide range of additional expert test and measurement services, which you can purchase according to your unique technical and business needs. Solve problems efficiently and gain a competitive edge by contracting with us for calibration, extra-cost upgrades, out-of-warranty repairs, and onsite education and training, as well as design, system integration, project management, and other professional engineering services. Experienced Agilent engineers and technicians worldwide can help you maximize your productivity, optimize the return on investment of your Agilent instruments and systems, and obtain dependable measurement accuracy for the life of those products.

Agilent Open

www.agilent.com/find/open
Agilent Open simplifies the process of connecting and programming test systems to help engineers design, validate and manufacture electronic products. Agilent offers open connectivity for a broad range of system-ready instruments, open industry software, PC-standard I/O and global support, which are combined to more easily integrate test system development.

United States:	**Korea:**
(tel) 800 829 4444	(tel) (080) 769 0800
(fax) 800 829 4433	(fax) (080)769 0900
Canada:	**Latin America:**
(tel) 877 894 4414	(tel) (305) 269 7500
(fax) 800 746 4866	**Taiwan**:
China:	(tel) 0800 047 866
(tel) 800 810 0189	(fax) 0800 286 331
(fax) 800 820 2816	**Other Asia Pacific**
Europe:	**Countries:**
(tel) 31 20 547 2111	(tel) (65) 6375 8100
Japan:	(fax) (65) 6755 0042
(tel) (81) 426 56 7832	Email: tm_ap@agilent.com
(fax) (81) 426 56 7840	Contacts revised: 05/27/05

For more information on Agilent Technologies' products, applications or services, please contact your local Agilent office. The complete list is available at:

www.agilent.com/find/contactus

Product specifications and descriptions in this document subject to change without notice.

© Agilent Technologies, Inc. 2005
Printed in USA, June 20, 2005
5989-3204EN

Agilent Email Updates

www.agilent.com/find/emailupdates
Get the latest information on the products and applications you select.

Agilent Technologies